Available online at www.sciencedirect.com
SCIENCE DIRECT®
Journal of Power Sources 119–121 (2003) 543–549
JOURNAL OF POWER SOURCES
www.elsevier.com/locate/jpowsour

The role of graphite surface group chemistry on graphite exfoliation during electrochemical lithium insertion

Michael E. Spahr[a,*], Henri Wilhelm[a], Tiziana Palladino[a], Nicole Dupont-Pavlovsky[b], Dietrich Goers[c], Felix Joho[c,1], Petr Novák[c]

[a]*TIMCAL SA, CH-6743 Bodio, Switzerland*
[b]*Laboratoire de Chimie du Solide Minéral-UMR 7555, Université de Nancy I, F-54506 Vandœuvre-lès-Nancy Cedex, France*
[c]*Laboratory for Electrochemistry, Paul Scherrer Institut, CH-5232 Villigen PSI, Switzerland*

Abstract

Heat treatment of highly crystalline graphite TIMREX® SLX50 at temperatures above 1200 °C in an inert gas atmosphere resulted in a significant increase of the irreversible capacity, which is observed during the first electrochemical lithium insertion using a 1 M $LiPF_6$ ethylene carbonate/dimethyl carbonate 1:1 (w/w) electrolyte mixture. An additional potential plateau could be observed at about 0.45 V versus Li/Li^+ during the galvanostatic insertion of lithium into these heat-treated graphite materials. *Post-mortem* scanning electron microscope studies of negative electrodes containing such heat-treated graphite materials indicated the exfoliation of the graphite structure as reason for the additional potential plateau and the significant increase of the irreversible capacity in the first electrochemical lithium insertion. The graphite exfoliation during the first electrochemical lithium insertion disappeared when the heat-treated graphite materials were aged in a humid air atmosphere at room temperature for several months. This aging process turned out to be reversible. When regenerating the aged graphite material in a dry flux of argon gas at room temperature, the electrochemical graphite exfoliation could be observed again. Structure characterization of the graphite materials by X-ray diffraction (XRD) as well as surface investigations using Raman spectroscopy and gas adsorption measurements indicated that the exfoliation tendency of polycrystalline, highly crystallized graphite in ethylene carbonate containing electrolytes is controlled neither by the rhombohedral stacking faults in the graphite structure, the surface defects, nor by the superficial disordered carbon but only by the surface group chemistry. The amount of acidic surface oxide groups especially seems to be the key factor that influences graphite exfoliation during electrochemical lithium insertion in ethylene carbonate containing electrolytes.

Keywords: Graphite surface groups; Graphite surface aging; Electrochemical graphite exfoliation; Electrochemical lithium insertion; Rechargeable lithium batteries

1. Introduction

The solid electrolyte interphase (SEI) layer, i.e. the passivation layer, which is formed in situ on the surface of the carbonaceous negative electrode material during the electrochemical lithium insertion from liquid electrolytes, is a key component in the negative electrode determining the electrochemical performance and safety aspect of the whole battery [1–5]. The formation of this passivation layer suppresses further electrolyte decomposition on the carbon surface. On the other side, the formation of the SEI-layer on the carbon surface contributes to the irreversible capacity during the first charging of the lithium-ion cell. This irreversible capacity leads to a reduction of the cell's energy density. An effective SEI-layer formation reduces the irreversible capacity in the first charge cycle of the cell and avoids battery failure due to decomposition reactions of the electrode material and electrolyte [6].

A prominent example is the incompatibility of polycrystalline graphite materials revealing high graphitization degrees in propylene carbonate-based electrolyte systems. These highly crystalline graphite materials allow high specific charges up to the theoretical capacity of 372 mAh/g corresponding to a chemical composition of LiC_6. During the electrochemical insertion of Li^+ from propylene carbonate-based electrolytes, the graphite structure of such graphite materials exfoliates leading to severe battery failure whereas graphite exfoliation can be avoided if propylene carbonate is replaced by, e.g. ethylene carbonate [7–9]. With the formation of an efficient SEI on the graphite particle surface in ethylene carbonate-based electrolyte systems, exfoliation can be suppressed.

* Corresponding author.
E-mail address: m.spahr@ch.timcal.com (M.E. Spahr).
[1] Present address: ESEC SA,CH-6330 Cham, Switzerland.

0378-7753/03/$ – see front matter
doi:10.1016/S0378-7753(03)00284-2

To achieve optimized SEI-layers, the electrolyte system must be adjusted to the individual carbon negative electrode material [10–13]. Recently, it has been shown that the crystal structure of the carbon negative electrode material as well as the carbon texture, porosity, and surface properties influences the formation of the SEI-layer [14–18]. However, usually it is very difficult to differentiate between the influences of the individual material properties in the experiment. The clear identification of the material parameter and its role in the SEI formation is an important factor for the further improvement of carbon negative electrode materials for lithium-ion batteries.

2. Experimental

TIMREX® SLX50 was heat-treated at different temperatures in an inert argon gas atmosphere for 2 h (argon purity 99.999%). The material was cooled down to room temperature under argon gas and then exposed to an air atmosphere. The storage of the material was performed in an air atmosphere at room temperature. The regeneration of the aged graphite materials was performed by exposing the material to a slight flux of argon at room temperature.

X-ray diffraction (XRD) measurements were performed on a PHILIPS PW1820 diffractometer using monochromatic Cu Kα radiation. The average crystallite size along the crystallographic *c*-axis direction, L_c, was determined from the (0 0 2) diffraction peak by using the Debye–Scherrer formula. The rhombohedral fraction was determined by comparing the respective intensities of the (1 0 1) hexagonal and rhombohedral peaks.

A confocal Raman microscope (Labram, DILOR/Instruments S.A.) was used to acquire Raman spectra of the graphite materials. Laser radiation at wavelength 530.9 nm emitted by a Kr^+ laser was used for excitation of Raman spectra in the range of about 1000–2300 cm^{-1}. The spectral resolution was approximately 4 cm^{-1}. Raman band positions were calibrated against the line spectrum of a neon lamp (PenRay, Oriel). The laser power applied to the sample was about 10 mW. Raman microscopy often reveals the heterogeneity of samples when investigated with focal zones of micrometer dimension. Therefore, an average spectrum was constructed from a Raman map, taking into account 144 single spectra recorded from electrode surface at a random position. This averaged Raman spectrum was used to calculate the intensity of the D- and the G-band in order to calculate the correlation length L_a [19,20]. It should be noted that the original Tuinstra–Koenig relation was established for a laser radiation wavelength of 514.5 nm. It is assumed that the optical properties of carbon materials are approximately the same, and that the Tuinstra–Koenig relation holds also at excitation wavelength of 530.9 nm.

Nitrogen adsorption was performed at liquid N_2 temperature (77.3 K) using a Micromeritics ASAP 2010. Krypton adsorption was performed at 77.3 K using a classical volumetric apparatus [21]. For the latter measurements, the samples were outgassed at 873 K until a residual pressure lower than 10^{-6} Torr had been reached. Thermal transpiration corrections were carried out according to the Takaishi and Sensui formula [22]. The evaluations of the measurements were performed according to [23].

Graphite pH-measurements were performed by dispersing 10 g graphite powder in 20 g ethanol and 170 g water. The pH-value of the dispersion was measured using a pH-meter with a combined calomel electrode (Metrohm, Herisau, Switzerland).

Electrochemical charge/discharge measurements were carried out at 25 °C in laboratory cells described elsewhere [24]. Metallic lithium was used as the reference and counter electrode. 1 M $LiPF_6$ in DMC/EC 1:1 (w/w) (Merck, Darmstadt, Germany) was used as the electrolyte solution. The graphite electrodes were prepared by blade coating of the graphite materials on a copper foil current collector. PVDF (Kynar 741, Elf Atochem, France) was used as binder material. For the electrochemical measurements, the coated graphite electrodes were dried under a reduced pressure of 10^{-3} mbar at 120 °C for 12 h. Electrochemical charge/discharge measurements were performed galvanostatically on Computer Controlled Cell Capture (CCCC, Astrol Electronic AG, Oberrohrdorf, Switzerland). We have chosen relatively low current densities of 10 mA/g of carbon to complete the SEI formation in the first Li^+ insertion cycle. After a potential of 5 mV versus Li/Li^+ was reached in the first galvanostatic Li^+ insertion, the discharging was continued potentiostatically until the specific current dropped below 5 mA/g. The electrochemical lithium de-insertion was performed at a constant current of 10 mA/g until a cut-off voltage of 1.5 V versus Li/Li^+ followed by a subsequent potentiostatic stabilization at this potential until the specific current dropped below 5 mA/g.

The double layer capacitance was calculated from the imaginary part of the impedance measured at 0.01 Hz. Impedance spectra were recorded at 2.5 V versus Li/Li^+ at a temperature of 298 K using a Solartron impedance spectrometer at an ac signal amplitude of 10 mV. The impedance spectra at 0.3 V versus Li/Li^+ were measured in cells that were galvanostatically discharged at 10 mA/g to 0.3 V versus Li/Li^+ and subsequently potentiostatically stabilized for 2d.

The same cells were used for the *post-mortem* scanning electron microscopy (SEM) studies. The cells were dismantled, the negative electrodes were washed thoroughly with dry DMC and dried in dry argon. SEM images were recorded with a JEOL JSM-5600 using a heated wolfram anti-cathode.

3. Results and discussion

Recently, we reported a significant increase of the irreversible capacity in the first electrochemical insertion of Li^+

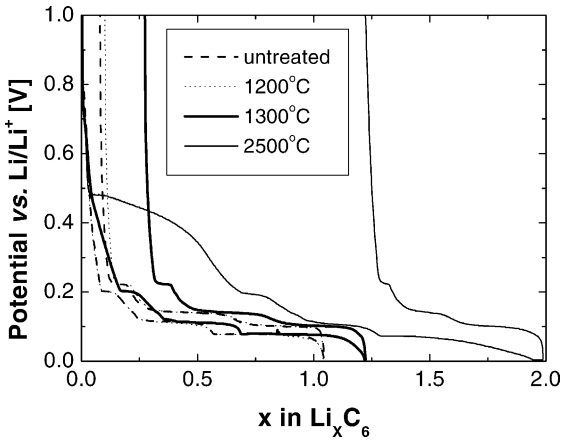

Fig. 1. First galvanostatic Li^+ insertion and de-insertion at 10 mA/g in TIMREX® SLX50, and TIMREX® SLX50 heat-treated at 1200, 1300 °C as well as 2500 °C in an inert gas atmosphere.

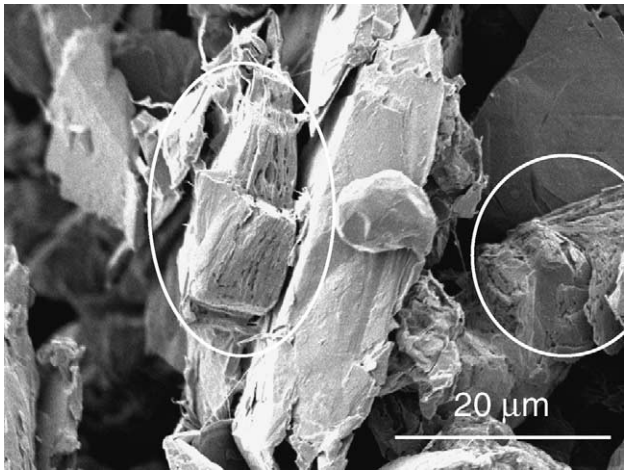

Fig. 2. Scanning electron microscope picture of an electrode containing TIMREX® SLX50 heat-treated at 2500 °C. The electrode was galvanostatically discharged to 0.3 V vs. Li/Li^+ at 10 mA/g and stabilized at 0.3 V vs. Li/Li^+ for 2d. The highlighted zones show slightly exfoliated graphite particles. The exfoliation is indicated by small holes and interspaces between the graphene layers at the prismatic surfaces of the graphite crystals.

from an ethylene carbonate-based liquid electrolyte in a graphite material, which had been heat-treated at 3000 °C in an inert gas atmosphere [23,25]. This increase of the irreversible capacity occurred despite of the fact that the specific BET surface area of the graphite decreased by the heat treatment. The increase of the irreversible capacity became apparent by an additional potential plateau in the electrochemical Li^+ insertion potential curve and was explained as graphite exfoliation. It could be shown that the amount of rhombohedral stacking defects did not have a direct influence on the irreversible capacity increase and the tendency of the graphite to exfoliate.

To identify the critical temperature leading to the deterioration of the electrochemical insertion properties of highly crystalline graphite, a more detailed study of the treatment temperature was performed. Fig. 1 shows the electrochemical lithium insertion properties of TIMREX® SLX50 being treated at various temperatures in an inert argon gas atmosphere. At temperatures above 1200 °C, the characteristic potential plateau at about 0.45 V versus Li/Li^+ could be observed in galvanostatic Li^+ insertion experiments using a 1 M $LiPF_6$ EC/DMC 1:1 (w/w) electrolyte. This potential plateau increased in size when the treatment temperature was further increased. A graphite material, which was treated at temperatures of 1200 °C and below, did not show this potential plateau.

To further investigate the origin of the additional potential plateau at 0.45 V versus Li/Li^+, *post-mortem* SEM investigations of heat-treated SLX50 graphite negative electrodes were performed. For theses studies, lithium half-cells equipped with such negative electrodes initially were galvanostatically discharged to 0.3 V versus Li/Li^+ and subsequently stabilized potentiostatically at this potential for 2 days. Fig. 2 shows, as an example, the SEM picture of a negative electrode containing SLX50, which was heat-treated at 2500 °C (SLX50 HT). Slight exfoliation of the graphene layers could be observed, indicated by small holes and interspaces between the graphene sheets at the prismatic surfaces of the graphite crystals. Impedance spectroscopic studies revealed an increase of the double layer capacitance from ca. 0.12 to about 66.3 F/g during the lithium insertion in the potential range between 2.5 and 0.3 V versus Li/Li^+ indicating a drastic increase of the electroactive electrode surface area after the electrode passed through the potential plateau at 0.45 V versus Li/Li^+. The potential plateau at about 0.45 versus Li/Li^+ describes the electrochemical exfoliation of the graphite structure. During the exfoliation process of the graphite electrode, the electrode surface area increases. Thus, the SEI-layer must be formed on a larger surface area compared to the non-exfoliated electrode, which explains the significant increase of the irreversible capacity during the exfoliation process.

Table 1 shows material parameters, which were obtained from XRD experiments as well as nitrogen and krypton gas adsorption experiments. These data characterize the changes of the crystal structure, texture and surface morphology during the heat treatment at different temperatures. The XRD patterns of the graphite materials indicated no significant change of the crystallinity and graphite texture at treatment temperatures up to 1300 °C. The coherent length of the graphite crystallites along the *c*-axis, L_c, as well as the amount of rhombohedral stacking faults stayed in the same range for graphite materials treated up to 1300 °C. Also no significant change of the graphite specific surface area could be detected up to this temperature, as it is indicated by the specific BET surface areas obtained from nitrogen adsorption experiments as well as by the surface areas obtained from krypton adsorption measurements. The latter surface areas were deduced from the amount of adsorbed krypton at the commensurate–incommensurate transition of the condensed krypton atom mono-layer on the graphite surface.

Table 1
Results of X-ray diffraction experiments and nitrogen and krypton gas adsorption experiments performed on TIMREX® SLX50, and TIMREX® SLX50 heat-treated at 1200, 1300 °C as well as 2500 °C in an inert gas atmosphere

Graphite sample	L_c (nm)	Rhombohedral fraction (%)	BET SSA (m^2/g) (N_2)	SSA (m^2/g) (Kr)	Polar edges (%)	Basal planes (%)	Low energy defects (%)
TIMREX® SLX50	360	23 (±2)	4.0	3.8	25	42	33
TIMREX® SLX50 (1200 °C)	340	23 (±2)	4.1	4.0	25	42	33
TIMREX® SLX50 (1300 °C)	380	20 (±2)	4.0	4.0	34	41	25
TIMREX® SLX50 (2500 °C)	600	0 (no rhombohedral diffraction peaks)	2.8	2.8	9	67	24

L_c values and rhombohedral fractions were measured by X-ray diffraction. The specific surface area was determined as a specific BET surface area using nitrogen gas adsorption. Specific surface areas from krypton adsorption experiments were deduced from the amount of krypton adsorbed at the commensurate–incommensurate transition of the condensed mono-layer of krypton atoms. The amounts of basal plane surfaces, prismatic surfaces, and low energy defects were calculated from the results of krypton adsorption measurements according to [23].

Interestingly, as a result of the krypton gas adsorption measurements, some low energy defects on the graphite surface were transformed into polar edges when increasing the treatment temperature from 1200 to 1300 °C.

A curing effect of the graphite structure, texture, and surface morphology could be observed when treating the graphite material under graphitization conditions at 2500 °C (SLX50 HT). The crystallinity of the graphite material increased which was reflected by a significant increase of the L_c value. The structural defects, i.e. the rhombohedral stacking faults completely vanished. Also the specific surface area of the graphite decreased significantly. The amount of prismatic surfaces on the graphite surface significantly decreased in favor of the amount of basal plane surfaces, which increased to the same extent whereas the fraction of low energy defects did not change compared to the graphite material treated at 1300 °C.

Raman spectroscopy used to characterize regions in particular near the graphite particle surface reflected a superficial crystallinity increase by a significantly increased L_a value caused by the graphite treatment at 2500 °C. Starting with the untreated TIMREX® SLX50 material ($L_a \approx 45$ nm), the crystallites grow up to the range of $L_a \approx 130$ nm for the graphite material heat-treated at 2500 °C. A very small additional shoulder with the center at about 1620 cm^{-1} (D″-band) could be observed in the Raman spectra of untreated graphite material only, probably due to smaller crystallite size or superficially oxidized graphite layers.

During storage of the heat-treated graphite materials under ambient conditions, the electrochemical insertion properties of the heat-treated graphite materials significantly changed with time. The potential plateau at 0.45 versus Li/Li^+ observed during the first electrochemical Li^+ insertion, i.e. the exfoliation of the graphene layers subsequently decreased with storage time and finally disappeared after a storage period of approximately 40–50 months, as shown in Fig. 3. This aging effect of the heat-treated material accelerated in the presence of some humidity in the air atmosphere to which the material was exposed.

This aging process of the graphite surface being observed appeared to be reversible. When exposing the heat-treated graphite materials, which were aged for an extended period of time until the electrochemical exfoliation vanished, to a slight dry argon stream at room temperature for some weeks, the graphite exfoliation in the first electrochemical Li^+ insertion appeared again (Fig. 4). Obviously, the aged

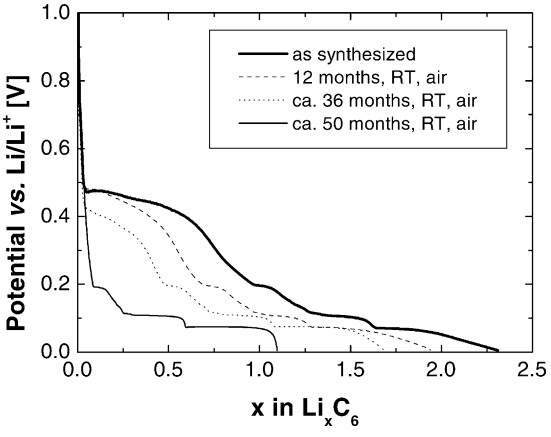

Fig. 3. First electrochemical Li^+ insertion at 10 mA/g in TIMREX® SLX50 heat-treated at 2500 °C in an inert gas atmosphere and aged in an ambient atmosphere at different times.

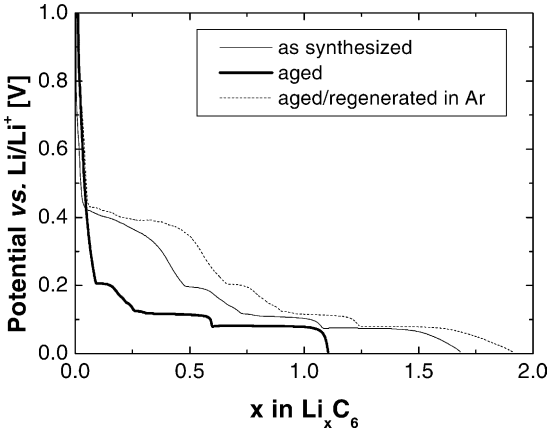

Fig. 4. First electrochemical Li^+ insertion in TIMREX® SLX50 heat-treated at 2500 °C in an inert gas atmosphere, aged in an ambient atmosphere for 50 months, and subsequently regenerated at room temperature under a dry argon stream (specific current: 10 mA/g).

graphite surface was regenerated in the argon flux. This regeneration effect could be accelerated when the aged graphite materials were exposed to dry argon at elevated temperature.

During the aging and regeneration process at room temperature, no change of the graphite's bulk crystallinity and texture was observed. We concluded that a surface effect, occurring during the storage of the heat-treated materials in air, must be responsible for the change of the electrochemistry. Obviously, the heat-treated graphite's surface is not stable in air but changes even at room temperature when exposed to an air atmosphere. The aging process of the heat-treated graphite surface in air seems to be reversible. Exposing the aged heat-treated graphite material to an argon atmosphere can reverse the modification of the graphite surface, which occurs during the aging reaction, leading to the regeneration of the graphite surface. Since the aging and regeneration of the graphite surface occurred at room temperature, it can be expected that it is predominantly the surface group chemistry which is modified during these processes.

Due to very low oxygen concentration on the graphite surface, it is difficult to apply even modern surface analytical methods (e.g. DRIFT, photoelectron spectroscopy) on graphite materials to detect changes of the surface functional groups which could explain the electrochemical behavior of the heat-treated graphite before and after the extended exposure to air. However, in the case of activated carbons and other less crystalline carbons with large surface areas, the behavior of the carbon surface chemistry during heat treatment and exposure to various gas atmospheres has been studied intensively and is well understood [26].

During the heat treatment in an inert gas atmosphere, most functional groups on the carbon surface are transformed into CO or/and CO_2 or/and H_2O at temperatures above 1200 °C [26–29]. After heat-treatment and cooling to room temperature, activated carbon materials are known to chemisorb oxygen when they are exposed to air or oxygen. The quantity of chemisorbed oxygen is relatively small and the oxygen species formed in this process seem to be involved in the basic surface properties of these carbon materials [29,30]. Basic surface oxides could also be the main surface groups for the SLX50 material which was treated under inert gas atmosphere above 1200 °C, subsequently cooled down and exposed to air atmosphere. pH-measurements of graphite dispersions in water delivered an indication of the change of the surface group chemistry during the heat-treatment. For the original SLX50 graphite material, a pH-value of 6.7 was obtained, whereas the pH increased to 9.0 in case of SLX50 being treated at 2500 °C under inert gas atmosphere.

In additional oxidation with oxygen or air at elevated temperatures or slower under room temperature conditions, the carbon surface acquires increasing acidic properties [31–34]. Activated carbons, which had been regenerated under vacuum or inert gas atmosphere were slowly oxidized by moist air at room temperature [34,35]. The formation of surface oxides at the carbon surface, which occurs during this aging process renders the carbon surface hydrophilic and has an adverse effect on the adsorption properties of such activated carbons [36]. These hydrophilic adsorption centers on the carbon surface are mainly represented by carboxylic or phenolic surface groups [30]. It has been shown in the literature that the presence of water vapor considerably enhances the surface oxidation of carbons at low temperatures [34,35,37]. Elevated temperatures above 60 °C shorten the aging process of the carbon surface [38]. Such an aging effect of the heat-treated graphite surface in an air atmosphere could be the explanation for the change of the electrochemical properties of heat-treated SLX50 graphite during storage in air. A modification of the heat-treated SLX50 graphite surface during storage in air at room temperature could be monitored experimentally by a decrease of the pH-value of the appropriate graphite dispersion. The aged heat-treated SLX50 (2500 °C), in which no exfoliation in the first electrochemical reduction could be observed, showed a pH of 6.4 indicating surface groups with more acidic properties.

Apparently, the surface oxides created by this aging process on the graphite surface seem to be weakly bound and decompose by treating the material in an inert gas stream at elevated temperatures or even room temperature with time. The lower amount of acidic surface oxides on the graphite surface increases the tendency of the graphite material to graphite exfoliation during the first electrochemical lithium insertion. However, the observed graphite regeneration process is quite surprising in that the time frame in which the regeneration process was observed is significantly shorter than the time frame of the aging process. In general, the kinetics of the oxygen chemisorption process on graphite follow the Elovitch law and exponentially decrease with increasing amount of adsorbed oxygen at constant temperature. Following this chemisorption mechanism, the surface oxide groups are generally too strongly bound to the surface to be removed by a simple flux of argon at room temperature. Moreover, if the activation energy of chemisorption produced such a slow aging, the desorption time should also be very long. An explanation could be that the aging originates from a contaminant present at a very low concentration in the sample environment leading to adsorbed species on the graphite surface which are able to desorb reversibly.

While Raman measurements clearly indicate a curing effect caused by the heat treatment of SLX graphite in an inert gas atmosphere at high temperatures, no changes of Raman spectra could be observed during the aging of the heat-treated graphite materials and the subsequent regenerating process in an argon gas stream (Fig. 5). The intensity of the D-band was very low for the heat-treated material and remained in the same range after the aging process. The amount of surface defects or disordered superficial carbon

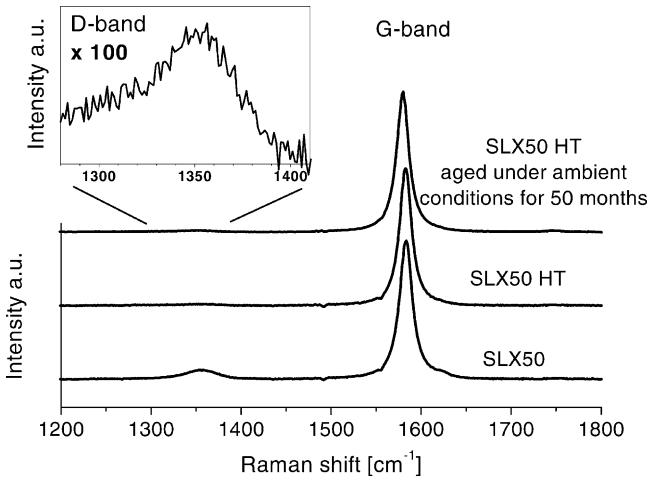

Fig. 5. Results of the Raman spectroscopic studies performed on TIMREX® SLX50, TIMREX® SLX50 heat-treated at 2500 °C (SLX50 HT) and TIMREX® SLX50 HT aged under ambient conditions for 50 months.

was affected neither by the aging process nor by the regeneration process of the aged graphite materials. It seems that only the surface chemistry changed during the processes, affecting the electrochemical properties of the heat-treated graphite and its tendency to exfoliate.

It must be pointed out that Raman spectroscopy is not able to verify changes of the composition and distribution of graphite surface groups which could be the reason for the observed electrochemical behavior. Besides, the laser power used could have damaged the graphite surface chemistry. Weakly bound or chemisorbed species could be especially affected by the irradiation of the laser. In addition, it is difficult to detect small changes of surface group species using Raman spectroscopy.

However, Raman spectroscopy is a sensitive tool to detect superficial disordered carbon and surface defects. Especially the surface defect concentration is directly related to the fraction of prismatic graphite surfaces. The amount of prismatic surfaces, and even more the amount of surface defects and superficial disordered carbon is directly linked to the amount of surface groups on the graphite surface but not necessarily to the nature of the surface groups. The results of the Raman investigation indicated that the amount of superficial disordered carbon and surface defects, i.e. the amount of prismatic surfaces, basal plane surfaces and low energy defects were not modified at room temperature during the aging of the heat-treated SLX50 in air or its subsequent regeneration in argon. It is more probable, that the surface group chemistry, i.e. the amount and nature of the graphite surface oxides, was affected by the aging and regeneration process of the heat-treated SLX50 graphite material. The obtained results indicate that in particular acidic surface oxides have a positive influence on the formation of an effective SEI-layer, which suppresses the tendency of graphite to exfoliate during the first electrochemical lithium insertion.

4. Conclusions

Graphite exfoliation effects occurring during the electrochemical Li^+ insertion in high crystalline graphite cannot only be observed in propylene carbonate containing electrolytes but also in electrolytes containing ethylene carbonate. These exfoliation effects can be generated by decreasing the amount of surface oxides at the polar edges of the graphite material. Such a graphite surface modification can be achieved by heating the material under inert gas at temperatures above 1200 °C. After exposing the heat-treated material to air, basic functional groups are formed. These basic functional groups apparently are not suitable to form an effective SEI-layer and thus are not able to avoid the exfoliation of the graphite negative electrode material. The aging of the graphite material in air leads to a further re-oxidation of the surface and most likely to the formation of acidic surface groups, which seem to be essential for an effective SEI-layer formation which is necessary to avoid the exfoliation of graphite in ethylene carbonate-based electrolytes. The surface groups, which are formed during the aging process in air are not stable in a dry inert gas atmosphere, i.e. the aging process can be reversed when the aged material is exposed to a stream of dry argon. This regenerated graphite material shows exfoliation during the first Li^+ insertion in ethylene carbonate containing electrolytes. The graphite crystal structure, i.e. the amount of rhombohedral stacking faults does not show a direct influence on the electrochemical phenomenon of graphite exfoliation. Also surface defects, superficial disordered carbon, or the degree of crystallinity near the graphite surface do not seem to be responsible for the formation of a SEI-layer on the graphite surface, which can effectively suppress electrochemical graphite exfoliation in ethylene-carbonate based electrolytes. Besides the choice of a suitable electrolyte, it is only the graphite surface chemistry, which decides whether the quality of the SEI-layer is sufficient to suppress the exfoliation of graphene layers during the electrochemical insertion of lithium ions in the graphite structure.

Acknowledgements

Numerous discussions with Dr. Hilmi Buqa (Paul Scherrer Institute) are gratefully acknowledged. Parts of this work were done under the auspices of the European research project PAMLiB-ENK6-CT1999-00013 supported by the European Community and the Swiss Federal Office of Education and Science.

References

[1] E. Peled, J. Electrochem. Soc. 126 (1979) 2047.
[2] J.R. Dahn, A.K. Sleigh, H. Shi, B.M. Way, W.J. Weydanz, J.N. Reimers, Q. Zhong, U. von Sacken, in: G. Pistoia (Ed.), Lithium

Batteries, New Materials, Developments and Perspectives, Elsevier, Amsterdam, 1994 (Chapter 1).
[3] E. Peled, D. Golodnitsky, J. Penciner, in: J.O. Besenhard (Ed.), Handbook of Battery Materials, Wiley-VCH, New York, 1999 (Chapter 6).
[4] E. Peled, in: G.P. Gabano (Ed.), Lithium Batteries, Academic Press, New York, 1983, p. 43.
[5] F. Joho, P. Novák, E. Spahr, J. Electrochem. Soc. 149 (8) (2002) A1020.
[6] D. Aurbach, M.D. Levi, E. Levi, A. Schechter, J. Phys. Chem. B 101 (1997) 2195.
[7] A.N. Dey, B.P. Sullivan, J. Electrochem. Soc. 117 (1970) 222.
[8] J.O. Besenhard, H.P. Fritz, J. Electroanal. Chem. 53 (1974) 329.
[9] R. Fong, U. von Sacken, J.R. Dahn, J. Electrochem. Soc. 137 (1990) 2009.
[10] D. Aurbach, B. Markovsky, I. Weissman, E. Levi, Y. Ein-Eli, Electrochim. Acta 45 (1999) 67.
[11] D. Aurbach, A. Zaban, Y. Ein-Eli, I. Weissman, O. Chusid, B. Markovsky, M. Levi, E. Levi, A. Schechter, E. Granot, J. Power Sources 68 (1997) 91.
[12] E. Peled, D. Golodnitsky, C. Menachem, D. Bar-Tow, J. Electrochem. Soc. 145 (10) (1998) 3482.
[13] Y. Ein-Eli, Electrochem. Solid-State Lett. 2 (5) (1999) 212.
[14] B. Simon, S. Flandrois, A. Fevrier-Bouvier, P. Biensan, Mol. Cryst. Liq. Cryst. 310 (1998) 333.
[15] B. Simon, S. Flandrois, K. Guerin, A. Fevrier-Bouvier, I. Teulat, P. Biensan, J. Power Sources 8182 (1999) 312.
[16] H. Huang, W. Liu, X. Huang, L. Chen, E.M. Kelder, J. Schoonman, Solid State Ionics 110 (1998) 173.
[17] F. Cao, I.V. Barsukov, H.J. Bang, P. Zalesky, J. Prakash, J. Electrochem. Soc. 147 (2000) 3579.
[18] K. Guerin, A. Fevrier-Bouvier, S. Flandrois, M. Couzi, B. Simon, P. Biensan, J. Electrochem. Soc. 146 (1999) 3660.
[19] F. Tuinstra, J.L. Koenig, J. Chem. Phys. 53 (1970) 1126.
[20] H. Wilhelm, M. Lelaurain, E. McRae, J. Appl. Phys. 84 (1998) 6552.
[21] A. Thomy, X. Duval, J. Regnier, Surf. Sci. Rep. 1 (1981) 1.
[22] T. Takaishi, Y. Sensui, Trans. Faraday Soc. 59 (1963) 2503.
[23] M.E. Spahr, H. Wilhelm, F. Joho, J.-C. Panitz, J. Wambach, P. Novák, N. Dupont-Pavlovsky, J. Electrochem. Soc. 149 (8) (2002) A960.
[24] P. Novák, W. Scheifele, F. Joho, O. Haas, J. Electrochem. Soc. 142 (8) (1995) 2544.
[25] M.E. Spahr, H. Wilhelm, F. Joho, P. Novák, ITE Letters on Batteries, New Technologies & Medicine, vol. 2, No. 3, 2001.
[26] H.P. Boehm, Carbon 40 (2002) 145–149.
[27] C.A. León y León, L.R. Radoviè, in: P.A. Thrower (Ed.), Chemistry and Physics of Carbon, vol. 24, Marcel Dekker, New York, 1994, pp. 213–310.
[28] I.C. Lewis, L.S. Singer, in: P.L. Walker, P.A. Thrower (Eds.), Chemistry and Physics of Carbon, vol. 17, Marcel Dekker, New York, 1981, pp. 1–88.
[29] H.P. Boehm, in: P. Delhës (Ed.), Graphite and Precursors, Gordon & Breach, Amsterdam, 2001, pp. 141–178.
[30] R. Burstein, A. Frumkin, Z. Phys. Chem. A 141 (1929) 219.
[31] H.R. Kryt, G.S. de Kadt, Kolloid Z. 47 (1929) 44.
[32] I.M. Kolthoff, J. Am. Chem. Soc. 54 (1932) 4473.
[33] B.R. Puri, in: Proceedingd of the 5th Biennial Conference on Carbon, Pennsylvania State University, vol. 1, Pergammon Press, Oxford, 1962, p. 165.
[34] B.H.M. Billinge, J.B. Docherty, M.J. Bevan, Carbon 22 (1) (1984) 83–89.
[35] F. Carrasco-Marin, J. Rivera-Utrilla, J.P. Jolly, C. Morena-Castilla, J. Chem. Soc. Faraday Trans. 92 (15) (1996) 2779–2782.
[36] R. Sappok, H.P. Boehm, Carbon 6 (1968) 283.
[37] J.C. Petit, Y. Bahaddi, Carbon 31 (1993) 821.
[38] T. Kuretzky, H.P. Boehm, Extended Abstracts, Carbon'94, International Carbon Conference, Granada, Spain, p. 262.